

Evolution and slow decay of an unusual narrow ring of relativistic electrons near $L \sim 3.2$ following the September 2012 magnetic storm

R. M. Thorne,¹ W. Li,¹ B. Ni,¹ Q. Ma,¹ J. Bortnik,¹ D. N. Baker,² H. E. Spence,³ G. D. Reeves,⁴ M. G. Henderson,⁴ C. A. Kletzing,⁵ W. S. Kurth,⁵ G. B. Hospodarsky,⁵ D. Turner,⁶ and V. Angelopoulos⁶

Received 6 May 2013; revised 30 May 2013; accepted 1 June 2013; published 26 July 2013.

[1] A quantitative analysis is performed on the decay of an unusual ring of relativistic electrons between 3 and 3.5 R_E , which was observed by the Relativistic Electron Proton Telescope instrument on the Van Allen probes. The ring formed on 3 September 2012 during the main phase of a magnetic storm due to the partial depletion of the outer radiation belt for $L > 3.5$, and this remnant belt of relativistic electrons persisted at energies above 2 MeV, exhibiting only slow decay, until it was finally destroyed during another magnetic storm on 1 October. This long-term stability of the relativistic electron ring was associated with the rapid outward migration and maintenance of the plasmopause to distances greater than $L = 4$. The remnant ring was thus immune from the dynamic process, which caused rapid rebuilding of the outer radiation belt at $L > 4$, and was only subject to slow decay due to pitch angle scattering by plasmaspheric hiss on timescales exceeding 10–20 days for electron energies above 3 MeV. At lower energies, the decay is much more rapid, consistent with the absence of a long-duration electron ring at energies below 2 MeV. **Citation:** Thorne, R. M., et al. (2013), Evolution and slow decay of an unusual narrow ring of relativistic electrons near $L \sim 3.2$ following the September 2012 magnetic storm, *Geophys. Res. Lett.*, 40, 3507–3511, doi:10.1002/grl.50627.

1. Introduction

[2] The twin NASA Van Allen probes were launched into highly elliptical, low inclination orbits on 30 August 2012, with the prime scientific objective of understanding the processes responsible for causing variability of the Earth's radiation belts. A moderate magnetic storm (with minimum

$Dst \sim -70$ nT) was already in progress, and the outer electron radiation belt was enhanced at $L > 3$ up to energies above 9 MeV when the Relativistic Electron Proton Telescope (REPT) instrument [Baker *et al.*, 2012] was first activated on 1 September. Search coil data from the Electric and Magnetic Field Instrument and Integrated Science (EMFISIS) [Kletzing *et al.*, 2013] was also available during this early period of instrument commissioning, allowing the following evolution of the radiation belt fluxes to be investigated in relation to both in situ whistler mode wave activity and the location of the plasmopause. An interplanetary shock hit the Earth's magnetosphere on 3 September, leading to a pronounced depletion of the outer zone fluxes at radial distance greater than 3.5 R_E and leaving a remnant ring of relativistic electrons behind between 3 and 3.5 R_E (Figure 1). This unusual radiation belt ring persisted with only modest decay until it was finally destroyed, together with the entire reformed outer zone (at $L > 4$) during another interplanetary shock passage on 1 October. The initial discovery of the ring was reported by Baker *et al.* [2013]. Here we describe the early evolution of the ring and provide a quantitative analysis of its slow decay inside the plasmasphere due to scattering by plasmaspheric hiss. We also explain why the long-duration ring is only observed at energies above 2 MeV.

2. Formation of the Ring and Early Recovery of the Outer Radiation Belt

[3] The dynamical variability of outer radiation belt relativistic electrons observed by REPT during the month of September 2012 is illustrated in Figures 1b–1d, together with the intensity of whistler mode chorus emissions (Figure 1f) and plasmaspheric hiss (Figure 1g), observed by the EMFISIS magnetic search coil instrument on both Van Allen probes. Since high-resolution wave burst data is limited to certain time intervals, we have constructed a robust scheme to separate the emissions into chorus and hiss for the standard wave spectrum data (6 s time resolution) based on their known properties. Here chorus magnetic wave amplitudes are calculated over the frequency range of $0.1\text{--}0.8 f_{ce}$, where f_{ce} is the equatorial electron cyclotron frequency, and hiss wave amplitudes are calculated by integrating wave spectral density between 100 Hz and 2 kHz. f_{ce} was calculated by mapping the local electron gyrofrequency measured from the EMFISIS magnetometer instrument to the magnetic equator using a dipole magnetic field model for simplicity. Following the passage of the interplanetary shock (Figure 1a) on 3 September, the plasmopause was displaced inward to $L \sim 3$, as indicated by the spatial distribution of

Additional supporting information may be found in the online version of this article.

¹Department of Atmospheric and Oceanic Sciences, University of California, Los Angeles, California, USA.

²Laboratory for Atmospheric and Space Research, University of Colorado Boulder, Colorado, USA.

³Institute for the Study of Earth, Oceans, and Space, University of New Hampshire, Durham, New Hampshire, USA.

⁴Space Science and Applications Group, Los Alamos National Laboratory, Los Alamos, New Mexico, USA.

⁵Department of Physics, University of Iowa, Iowa City, Iowa, USA.

⁶Department of Earth and Space Sciences, University of California, Los Angeles, California, USA.

Corresponding author: R. M. Thorne, Department of Atmospheric and Oceanic Sciences, University of California, 405 Hilgard Ave., Los Angeles, CA 90095, USA. (rmt@atmos.ucla.edu)

©2013. American Geophysical Union. All Rights Reserved.
0094-8276/13/10.1002/grl.50627

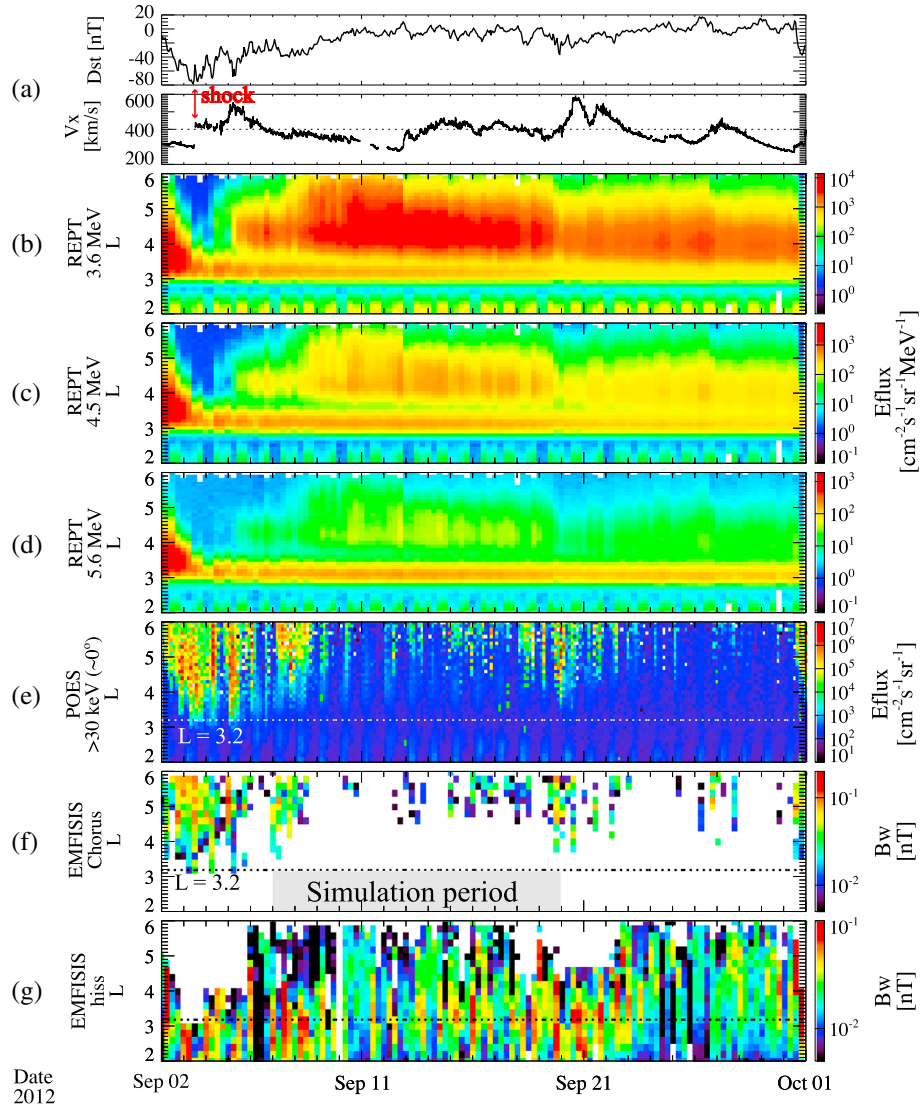


Figure 1. (a) The Dst index and solar wind velocity during September 2012. (b–d) Evolution of energetic electron flux at 3.6, 4.5, and 5.6 MeV showing the development and long-term stability of the unusual third radiation belt ring between 3.0 and 3.5 R_E , measured by the REPT instrument on the Van Allen probes. (e) >30 keV electron precipitation flux on the nightside (21–03 MLT) obtained from multiple POES satellites. (f) RMS magnetic wave amplitudes of chorus emissions, averaged over $\Delta L = 0.2$ and 6 h, obtained by the EMFISIS search coil magnetometers on both Van Allen probes A and B. (g) Similar RMS amplitudes of plasmaspheric hiss from EMFISIS.

both chorus emissions, which are generated in the low density region outside the plasmapause [Meredith *et al.*, 2012], and hiss, which is confined inside the plasmapause [Meredith *et al.*, 2004]. These observations from the two Van Allen probes were obtained near dawn and on the dayside. However, an approximate location of the plasmapause on the nightside can also be inferred from the precipitation flux of low energy electrons (> 30 keV) obtained from the Medium Energy Proton and Electron Detector (MEPED) on board the NOAA POES spacecraft [Evans and Greer, 2004] over 21–03 MLT (Figure 1e), since it has been demonstrated that this precipitation is caused by resonant scattering by chorus [Thorne *et al.*, 2010; Ni *et al.*, 2011]. All three proxies indicate that the plasmapause location was confined to $L < 4$ until 5 September, when there was an outward migration to $L > 5$. There was a further inward migration (to

$L \sim 4$) of both chorus emissions observed by EMFISIS on the dayside, and > 30 keV electron precipitation on the nightside on 7 September and later on 19 September, but throughout this interval, the ring of relativistic electrons was located well inside the plasmasphere and was therefore protected from the highly dynamic changes occurring in the outer radiation belt [e.g., Thorne, 2010] at $L > 4$.

[4] The development and persistence of the isolated ring of electrons between 3 and 3.5 R_E were only clearly evident in REPT data at energies above 2 MeV [Baker *et al.*, 2013]. However, there is evidence from the THEMIS spacecraft [Angelopoulos, 2008] of the formation of a ring of electrons peaking near $L \sim 3.5$ on 3 September at energies below 1 MeV. This lower energy ring decayed rapidly in less than a day and was absorbed between 4 and 5 September within the reforming outer zone (Figure 3b). There was also a rapid

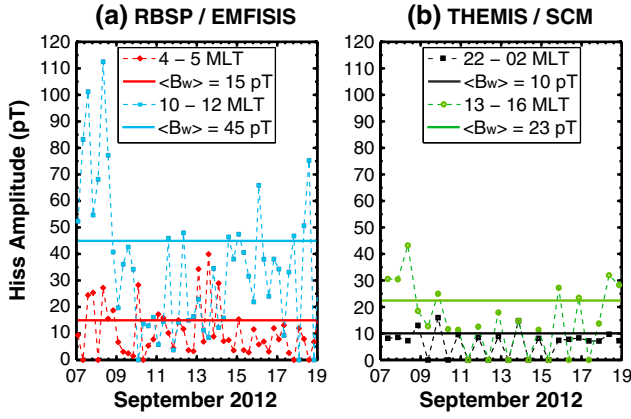


Figure 2. The RMS amplitudes of plasmaspheric hiss, averaged over the range $3.0 < L < 3.5$, at different MLT measured by the search coil magnetometers on (a) Van Allen probes (EMFISIS instrument) and (b) THEMIS (SCM instrument) spacecraft during the interval 7–19 September 2012. The RMS wave amplitudes of hiss over the entire interval in the different MLT sectors are indicated by the solid horizontal lines.

reformation of the more energetic outer radiation belt at $L > 4$ beginning early in the storm recovery on 4 September (Figure 1b). This rebuilding of the outer belt was most rapid at lower energies and occurred in the region outside the plasmapause over the range of L -shells where chorus emissions were observed to be strong, consistent with local wave acceleration [e.g., Horne and Thorne, 2003; Horne et al., 2005; Turner et al., 2013]. The complex dynamical processes responsible for the early evolution of the ring and the rebuilding of the outer zone during the recovery phase of the September storm are well beyond the scope of the present study and will be treated in a separate paper. Instead, we concentrate our attention here on the slow decay of the relativistic electron ring during the interval between 7 and 19 September (shaded in Figure 1f) when the radiation belt ring was located well inside the plasmapause. We show that the slow decay is caused by pitch angle scattering due to plasmaspheric hiss, using wave data obtained on the two Van Allen probes and on the three inner THEMIS spacecraft.

3. Simulation of the Decay of the Relativistic Electron Ring Near $L = 3.2$

[5] Over the time interval between 7 and 19 September, when the energetic electrons in the ring between 3.0 and 3.5 R_E are located deep within the plasmasphere, their dynamics will be primarily controlled by resonant interactions with plasmaspheric hiss [e.g., Abel and Thorne, 1998]. To evaluate the average rates of scattering as a function of energy and pitch angle, a global model must be constructed for the power spectral intensity and wave normal distribution of hiss. Figure 2 shows the temporal variability of the Root Mean Square (RMS) magnetic wave amplitude of plasmaspheric hiss obtained at each 6 h time bin observed on each satellite pass over the radial range $3.0 < L < 3.5$ by the search coil magnetometers from the EMFISIS instrument on the two Van Allen probes and from the three THEMIS

spacecraft over the time interval of interest. The data from multiple spacecraft provide good coverage over a broad range of MLT. Despite the considerable variability, this allows us to construct a global model for the RMS wave amplitudes of hiss in each range of MLT, shown by the solid horizontal lines. Notice that hiss is much stronger on the dayside, consistent with earlier statistical analyses [e.g., Meredith et al., 2004]. For the wave normal distribution and its variation with latitude below 45° , we adopt a realistic model (see supporting information) based primarily on ray tracing [e.g., Bortnik et al., 2011], which is consistent with observations of hiss [Santolík et al., 2001; Agapitov et al., 2012]. The average wave parameters over four MLT intervals (Table 1) are then used to evaluate the drift and bounce-averaged quasi-linear pitch angle diffusion coefficients shown in Figure 3a as a function of electron energy and equatorial pitch angle at $L \sim 3.2$. A dipole magnetic field and the plasmaspheric density model of Sheeley et al. [2001] are adopted. The wave spectral intensity and electron number density are assumed to remain constant along the field line. The diffusion coefficient calculations include contributions from the $N = -10$ to $N = 10$ cyclotron harmonic resonances and the Landau resonance $N = 0$.

[6] The timescale associated with scattering at high pitch angles is clearly comparable to or less than a day for energies below 2 MeV (Figure 3a). Furthermore, since the observed hiss amplitudes are much larger during the early phase of the storm recovery prior to 9 September (Figure 2 and Figure 1g), the scattering during this period should be much faster, and we should expect a relatively rapid redistribution of the lower energy population, as shown by the THEMIS data (Figure 3b) and consistent with the absence of a noticeable long-duration electron ring in REPT data below 2 MeV [Baker et al., 2013]. In contrast, the average scattering times of electrons with pitch angles above 70° (where the flux peaks) exceed 5–10 days above 3.6 MeV and increase with energy. Consequently, the scattering of the high-energy population is relatively slow, allowing the unusual electron ring to persist at energies above 4.5 MeV until it was finally destroyed during another storm on 1 October (Figure 1).

[7] To quantify the temporal evolution of the high-energy electrons, we have used the average diffusion rates shown in Figure 3a to solve the pure pitch angle diffusion equation for the temporal change of the electron flux as a function of pitch angle for three representative energies. The initial conditions are taken from an average of REPT observations over the radial range 3.0–3.5 on 7 September, and further details of the simulation are provided in the supporting information.

Table 1. RMS Hiss Wave Amplitude in Four MLT Intervals, Based on the Search Coil Magnetometers From the EMFISIS Instrument on the Van Allen Probes and From the THEMIS Spacecraft, and the Adopted Gaussian Wave Frequency Parameters Used for Quasi-Linear Diffusion Coefficient Calculations [e.g., Abel and Thorne, 1998]

	MLT Coverage of Hiss Emissions			
	22–02	02–06	06–14	14–22
Bw (pT)	10	15	45	23
Drift averaging	1/6	1/6	1/3	1/3
Hiss Wave Frequency Spectrum				
f_{ic} (Hz)	f_{uc} (Hz)	f_m (Hz)	δf (Hz)	
100	2000	550	300	

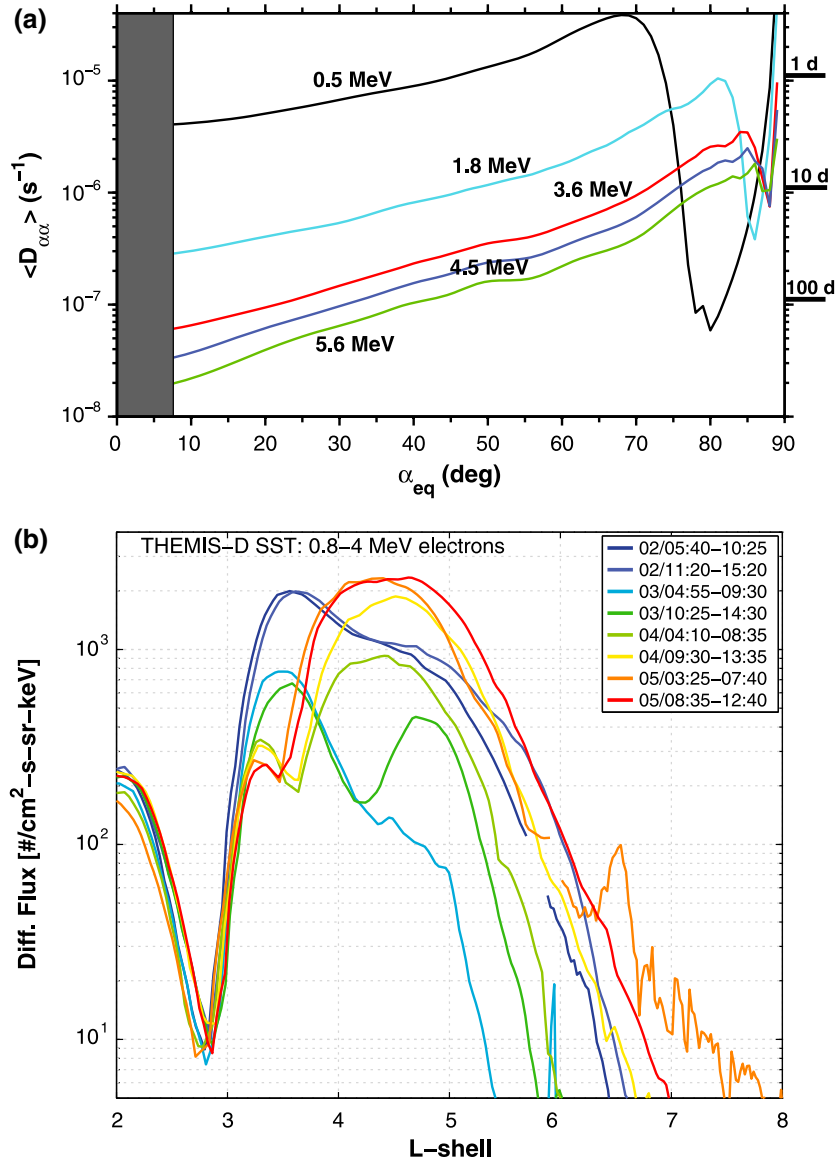


Figure 3. (a) Bounce and drift averaged rates of pitch angle diffusion obtained using a global model for the average properties of plasmaspheric hiss over the period 7–19 September 2012. (b) The spatial distribution of energetic electrons (0.8–4 MeV) observed on THEMIS D showing the rapid decay at $L > 3.5$ on the inbound pass on 3 September (04:55–09:30 UT) followed by an equally rapid rebuilding of the outer zone leading to two separate peaks in flux at $L \sim 3.5$ and $L \sim 4.7$ on the following outbound pass on 3 September (10:25–14:30 UT). The inner peak (inside $L = 3.5$) exhibits rapid decay and is absorbed within the growing outer radiation belt between 4 and 5 September.

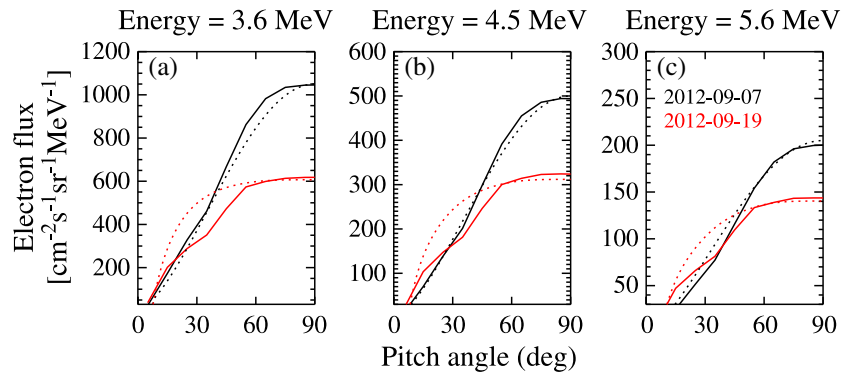


Figure 4. Comparison between the measured (solid) and simulated (dotted) decay of the electron flux between 7 and 19 September as a function of pitch angle for three REPT energies.

A comparison of the simulation (dotted lines) with the pitch angle distributions observed by REPT (solid lines) is shown in Figure 4. Although there are some differences between the simulation and observations at pitch angles below 60° , which could be due to either the limited angular resolution of the data or our assumptions on the latitudinal distribution of the waves, the numerical simulations reproduce the slow decay of the peak flux near 90° and also indicate that the electrons are transported toward the loss cone on a timescale that increases with electron energy.

4. Discussion and Conclusions

[8] A quantitative analysis has been made of the scattering of highly relativistic electrons in an unusual isolated ring, which formed between 3.0 and 3.5 R_E following a magnetic storm in early September 2012. We demonstrate that the slow temporal decay of the electron ring for energies above 3 MeV is caused by pitch angle scattering due to the global distribution of plasmaspheric hiss observed by search coil magnetometers on the two Van Allen probes and the three inner THEMIS spacecraft. Our analysis also explains why the long-duration third radiation belt ring is not observed at electron energies below 2 MeV, since the scattering decay timescales at these lower energies are comparable to a day or less. It is important to realize that the decay rates measured by REPT and simulated in the present work correspond to injected relativistic electron fluxes with equatorial pitch angles larger than $\sim 45^\circ$. The timescale for loss to the atmosphere would be much longer, typically > 100 days for energies above 3.6 MeV. Our rates of pitch angle diffusion shown in Figure 3a are comparable to those used by Meredith *et al.* [2009] to account for loss of 2 MeV electrons observed on SAMPEX in the outer portion of the slot region near $L \sim 3$. However, the timescales quoted by Meredith *et al.* [2009] only apply to losses after the electrons reach an equilibrium pitch angle distribution and are much longer than the timescale for initial redistribution of equatorially trapped flux treated here.

[9] Evidence for the formation of a double-peaked distribution of outer belt electrons during magnetic storm conditions has recently been reported from the analysis of THEMIS data [Turner *et al.*, 2013]. It thus appears that conditions under which this third radiation belt formed are not that unusual. It required the acceleration of outer zone relativistic electrons down to radial locations normally associated with the slot or gap between the inner and outer radiation belts [Lyons and Thorne, 1973] followed by a rapid loss from the outer portion of the outer belt and a rapid outward migration of the plasmopause. This left the remnant relativistic ring well inside the plasmasphere, where it was immune from the highly dynamical processes occurring in the low-density region outside the plasmopause. The unprecedented high-resolution data available from the REPT instrument, together with the slow decay at energies above 2 MeV, allowed us to monitor the evolution of this third radiation belt as a function of energy and quantify that the slow decay is caused by pitch angle scattering by observed amplitudes of plasmaspheric hiss.

[10] **Acknowledgments.** This work was supported by JHU/APL contracts 967399 and 921647 under NASA's prime contract NAS5-01072. The analysis at UCLA was supported by EMFISIS sub-award 1001057397:01 and by ECT sub-award 13-041. The authors acknowledge NASA contract NAS5-02099 and A. Roux and O. LeContel for use of the SCM data. We thank OMNIweb for providing the geomagnetic indices and solar wind parameters used in this study and the NOAA POES team for providing the POES electron data.

References

- Abel, R. W., and R. M. Thorne (1998), Electron scattering loss in Earth's inner magnetosphere, 1: Dominant physical processes, *J. Geophys. Res.*, **103**, 2385–2396.
- Agapitov, O., V. Krasnoselskikh, Y. V. Khotyaintsev, and G. Rolland (2012), Correction to "A statistical study of the propagation characteristics of whistler waves observed by Cluster," *Geophys. Res. Lett.*, **39**, L24102, doi:10.1029/2012GL054320.
- Angelopoulos, V. (2008), The THEMIS Mission, *Space Sci. Rev.*, **141**(1–4), 5–34, doi:10.1007/s11214-008-9336-1.
- Baker, D. N., et al. (2012), The relativistic electron-proton telescope (REPT) instrument on board the Radiation Belt Storm Probes (RBSP) spacecraft: Characterization of Earth's radiation belt high-energy particle populations, *Space Sci. Rev.*, doi:10.1007/s11214-012-9950-9.
- Baker, D. N., et al. (2013), A long-lived relativistic electron storage ring embedded in Earth's outer Van Allen belt, *Science*, **340**(6129), 186–190, doi:10.1126/science.1233518.
- Bortnik, J., L. Chen, W. Li, R. M. Thorne, N. P. Meredith, and R. B. Horne (2011), Modeling the wave power distribution and characteristics of plasmaspheric hiss, *J. Geophys. Res.*, **116**, A12209, doi:10.1029/2011JA016862.
- Evans, D. S., and M. S. Greer (2004), *Polar Orbiting Environmental Satellite Space Environment Monitor-2: Instrument descriptions and archive data documentation*, version 1.4, NOAA Tech. Mem. 93, Space Weather Predict. Cent., Boulder, Colo.
- Horne, R. B., and R. M. Thorne (2003), Relativistic electron acceleration and precipitation during resonant interactions with whistler-mode chorus, *Geophys. Res. Lett.*, **30**(10), 1527, doi:10.1029/2003GL016973.
- Horne, R. B., et al. (2005), Wave acceleration of electrons in the Van Allen radiation belts, *Nature*, **437**, 227–230.
- Kletzing, C. L., et al. (2013), The Electric and Magnetic Field Instrument Suite and Integrated Science (EMFISIS) on RBSP, *Space Sci. Rev.*, doi:10.1007/s11214-013-9993-6.
- Lyons, L. R., and R. M. Thorne (1973), Equilibrium structure of radiation belt electrons, *J. Geophys. Res.*, **78**, 2142–2149.
- Meredith, N. P., R. B. Horne, R. M. Thorne, D. Summers, and R. R. Anderson (2004), Substorm dependence of plasmaspheric hiss, *J. Geophys. Res.*, **109**, A06209, doi:10.1029/2004JA010387.
- Meredith, N. P., R. B. Horne, S. A. Glauert, D. N. Baker, S. G. Kanekal, and J. Albert (2009), Relativistic electron loss timescales in the slot region, *J. Geophys. Res.*, **117**, A03222, doi:10.1029/2008JA013889.
- Meredith, N. P., R. B. Horne, A. Sicard-Piet, D. Boshier, K. H. Yearby, W. Li, and R. M. Thorne (2012), Global models of lower band and upper band chorus from multiple satellite observations, *J. Geophys. Res.*, **117**, A10225, doi:10.1029/2012JA017978.
- Ni, B., R. M. Thorne, N. P. Meredith, R. B. Horne, and Y. Shprits (2011), Resonant scattering of plasma sheet electrons leading to diffuse auroral precipitation: 2. Evaluation for whistler-mode chorus waves, *J. Geophys. Res.*, **116**, A04219, doi:10.1029/2010JA016233.
- Santolik, O., M. Parrot, L. R. O. Storey, J. S. Pickett, and D. A. Gurnett (2001), Propagation analysis of plasmaspheric hiss using Polar PWI measurements, *Geophys. Res. Lett.*, **28**, 1127–1130, doi:10.1029/2000GL012239.
- Sheeley, B. W., M. B. Moldwin, H. K. Rassoul, and R. R. Anderson (2001), An empirical plasmasphere and trough density model: CRRES observations, *J. Geophys. Res.*, **106**(A11), 25,631–25,641.
- Thorne, R. M. (2010), Radiation belt dynamics: The importance of wave-particle interactions, *Geophys. Res. Lett.*, **37**, L22107, doi:10.1029/2010GL044990.
- Thorne, R. M., B. Ni, X. Tao, R. B. Horne, and N. P. Meredith (2010), Scattering by chorus waves as the dominant cause of diffuse auroral precipitation, *Nature*, **467**, 934–936, doi:10.1038/nature09467.
- Turner, D. L., V. Angelopoulos, W. Li, M. D. Hartinger, M. Usanova, I. R. Mann, J. Bortnik, and Y. Shprits (2013), On the storm-time evolution of relativistic electron phase space density in Earth's outer radiation belt, *J. Geophys. Res. Space Physics*, **118**, 2196–2212, doi:10.1002/jgra.50151.